SUPPLEMENTARY MATERIALS

SUPPLEMENTARY METHODS

Antibody Purification

LBH antibody (Lindley and Briegel, 2013) was affinity-purified as follows: recombinant HPLC-purified LBH protein (10 µg) (Al-Ali et al., 2010) was separated on a 15% SDS-PAGE gel and transferred to BA85-nitrocellulose membrane (Schleicher-Schuell). The nitrocellulose membrane was stained with Ponceau Red (Sigma) to facilitate visualization and excision of the LBH-specific protein band. The LBH protein-containing nitrocellulose strip was treated with 100 mM glycine/HCl pH 2.5 for 5 min and washed 2 x 2 min in Tris-buffered saline/TBS (20 mM Tris-HCl pH 7.4, 137 mM NaCl, 5 mM KCl, 0.7 mM $CaCl_2$, 0.5 mM $MgCl_2$, 0.6 mM Na_2HPO_4) to remove excess unbound protein. After blocking in TBS plus 3% BSA, the membrane was incubated overnight with 50 µl of rabbit polyclonal LBH anti-serum diluted in 350 µl TBS. Unspecific bound IgG's were removed by washing the membrane with TBS 3 x 5 min. LBH-specific IgG's were eluted by applying 30 µl of 100 mM glycine/HCl pH 2.5 to the nitrocellulose strip at room temperature (RT) for 10 min in a 0.7 ml microfuge tube. A small hole was punched into the membrane-containing tube, placed inside a 1.5 ml microtube containing 10 µl of 1 M Tris pH 8.0, and centrifuged at 4,500 g at RT for 5 min to collect and neutralize the LBH-specific IgG eluate. This elution step was repeated with additional 10 µl of 100 mM glycine/HCl pH 2.5. Sodium azide and BSA were added at a final concentration of 5 mM and 1 mg/ml, respectively, to maintain antibody stability.

Mammary cell preparation

Mammary glands (pairs #3-5) were dissected from female mice at 7 - 9 weeks-of-age, minced with a scalpel and placed in 3 ml dissociation medium (EpicultB + supplements [Stemcell Technologies], containing 20 ng/ml EGF, 20 ng/ml FGF, 4 µg/ml Heparin, 5% heat-inactivated FBS/HI-FBS [Invitrogen], and 1 x collagenase/hyaluronidase [Stemcell Technologies]). Minced glands were dissociated for 6 hours (CD24-CD29 analyses) or overnight (Sca1/CD49b analyses) at 37°C with agitation. Resulting organoids were treated with 5 ml 0.8% NH_4Cl+0.1 mM EDTA (Stemcell Technologies) for 1 min to lyse red blood

cells, followed by 8 ml of 0.25% Trypsin-EDTA (Invitrogen) for 3 min, and 2 ml of 5 mg/ml dispase+1 mg/ml DNase (Stemcell Technologies) for 1-2 min, with pelleting of organoids between each treatment by 5 min centrifugation at 450g. The cell pellets were diluted in 8 ml of Hank's balanced salt solution (Stemcell Technologies) plus 2% HI-FBS, filtered through a 40 µm filter (BD Falcon) and, after centrifugation at 450 g for 5 min, resuspended in 1 ml of PBS+2% HI-FBS**.** To ensure single cell suspensions, cells were mechanically dissociated using a 25-gauge needle syringe.

Cell lines, and RNAi

MCF10A, a spontaneously immortalized human mammary epithelial cell line (Debnath et al., 2003), was obtained from the American Type Cell Collection (ATCC). 226L cells, which were derived from normal human mammoplasty tissues after FACS-sorting for luminal cell surface markers and experimental immortalization with hTERT (Shaw et al., 2012), were kindly provided by Dr. Robert Clarke, University of Manchester, UK. These MEC lines were grown in HuMEC medium (Invitrogen) and transiently transfected with 100 nM scrambled control or *Lbh*-specific Smartpool siRNAs (Dharmacon) using Dharmafect #1 transfection reagent for 3 days according to the manufacturer's protocol. HC11-vector and HC11-LBH cells were previously derived by stable transfection of HC11, a clonal mouse mammary epithelial cell line derived from pregnant CommaD/Balb6 mammary glands (Ball et al., 1988), with pCDNA3 or pCDNA3-LBH plasmids (Rieger et al., 2010) and grown in RPMI containing 10% FBS, 1% penicillin-streptomycin, 1 µg/ml EGF (Invitrogen), 5 µg/ml insulin (Sigma-Aldrich), and 200 µg/ml G418 (Invitrogen). All cell lines were maintained in a 5% CO_2-humidified incubator at 37°C.

SUPPLEMENTARY REFERENCES:

Ball, R. K., Friis, R. R., Schoenenberger, C. A., Doppler, W. and Groner, B. (1988). Prolactin regulation of beta-casein gene expression and of a cytosolic 120-kd protein in a cloned mouse mammary epithelial cell line. *Embo J* 7, 2089-2095.

Debnath, J., Muthuswamy, S. K. and Brugge, J. S. (2003). Morphogenesis and oncogenesis of MCF-10A mammary epithelial acini grown in three-dimensional basement membrane cultures. *Methods* 30, 256-268.

SUPPLEMENTARY TABLES

Table S1: List of qPCR primers

qPCR Primer	Sequence: 5'-3'
Mouse *Gapdh* forward	CCAGCCTCGTCCCGTAGACA
Mouse *Gapdh* reverse	TGTGCCGTTGAATTTGCCGT
Mouse *Lbh* forward	GAGATCGGCTGAGATGACC
Mouse *Lbh* reverse	CTTCAGTGGGTTCCACCAC
Mouse *Esr1* forward	TGTTGGATGCTGAACCGCCCA
Mouse *Esr1* reverse	AGTCCCCAAAGCCTGGCACT
Mouse *Keratin 5* forward	AGTGCAGGCTGAGTGGGGAA
Mouse *Keratin 5* reverse	ACCAGCAAAGCCGCTGCCAAG
Mouse *Keratin 8* forward	AGCTCGCTCTCGAACCTCCGT
Mouse *Keratin 8* reverse	TGGAAGAGCTGATGCGGGCAC
Mouse *Axin2* forward	TTTGGCACAGCTAGAGGAAG
Mouse *Axin2* reverse	TGGCTCTTTGTGATCTTCTGG
Mouse *ΔNp63* forward	GAAGATTCGCAGCGCAAGGCT
Mouse *ΔNp63* reverse	AGTGAGACTGGTCAAGGCTGCTCTC
Mouse *TAp63* forward	CCCTATTGCTTTCAGCCTCCTGGC
Mouse *TAp63* reverse	GCTGGGGTTTCTATGAAACGCTGGA
Mouse *Gata3* forward	AGGTATCCTCCGACCCACCAC
Mouse *Gata3* reverse	GCCAGAGAAGAGGATGAAGCCG
Mouse *Slug* forward	TCAACGCCTCCAAGAAGCCCA
Mouse *Slug* reverse	ATAGGGCTGTATGCTCCCGAGGT
Human *GAPDH* forward	ATCAAGTGGGGCGATGCTG
Human *GAPDH* reverse	ACCCATGACGAACATGGGG
Human *LBH* forward	TCACTGCCCCGACTATCTG
Human *LBH* reverse	GGTTCCACCACTATGGAGG
Human *ESR1* forward	CCGCAGCTGTCGCCTTTCCT
Human *ESR1* reverse	TCTGCCACCCTGGCGTCGAT
Human *ΔNp63* forward	TCCTGGAGCCAGAAGAAAGGACAGC
Human *ΔNp63* reverse	CCA GGTTCGTGTACTGTGGCTCACT
Human *TAp63* forward	TTCACGGTGTGCCACCCTACAGT
Human *TAp63* reverse	TGCTCTGGGACATGGTGGATCGG

SUPPLEMENTARY FIGURE LEGENDS

Fig. S1. Expression of *Lbh* is restricted to GFP$^+$ stem cells in *Lgr5-EGFP-CreER^{T2}* mammary glands. (A) The Lin-negative cell fraction (Lin: CD45/CD31/TER119) of primary mammary cells from *Lgr5-GFP-CreER^{T2}* mice were FACS-sorted into GFP$^-$CD24^{hi} and GFP$^+$CD24$^+$ subpopulations. A representative FACS dot plot is shown. (B) qPCR analysis of *K8* and *K5* expression shows that GFP$^-$ CD24^{hi} are luminal and GFP$^+$CD24$^+$ basal cells, respectively. (C) Mammosphere assays showing significantly increased sphere formation by the GFP$^+$CD24$^+$ cell fraction relative to the GFP$^-$CD24^{hi} fraction (>3 fold; ***p<0.01*, n=3), indicating it is enriched in stem/progenitor cells. (D) qPCR analysis of sorted cells shows predominant expression of *Lbh* and the WNT target gene *Axin2* in the GFP$^+$CD24$^+$ MaSC subpopulation (*p<0.01*). Values were normalized to *Gapdh* and represent means ± SEM (n=3 female mice).

Fig. S2: Normal mammary gland morphogenesis and growth in epithelial-specific *Lbh*–deficient mice at pre- and post-pubertal stages. (A, B) Whole mount images of mammary glands from pre-pubertal 4 week/wk-old (A) and post-pubertal 11 wk-old (B) *K14-Cre;Lbh$^{+/}$* WT and *K14-Cre;Lbh$^{loxP/loxP}$* females (n=3 per genotype). *Lbh*-deficient mammary glands exhibit normal TEB formation at 4 weeks of age (arrows), as well as normal morphology at both of these stages except for slightly reduced side branching. Scale bars: 1 mm.

Fig. S3: Epithelial-specific LBH ablation impairs parity-induced lobulo-alveolar expansion, accompanied by reduced cell proliferation and precocious lactogenic differentiation. (A) Representative images of carmine red-stained whole mounts and H&E-stained sections of mammary glands from *K14-Cre;Lbh$^{+/+}$* WT and *K14-Cre;Lbh$^{loxP/loxP}$* females at day 12.5 (D12.5) of pregnancy and day 1 (D1) of lactation (n=2 per genotype). Note the abnormal presence of milk droplets (black arrow) in pregnant *Lbh*-deficient glands. Scale bars: 1 mm (black); 25 μM (red). (B) Normal lactation of *K14-Cre;Lbh$^{loxP/loxP}$* mutant mice as determined by daily assessment of the average weight of pups from birth to lactation day 15 (n=2 females per genotype). (C) IHC analysis of mid-pregnant (D12.5) *K14-Cre;Lbh$^{+/+}$*

WT and *K14-Cre*;*Lbh*$^{loxP/loxP}$ glands for Ki67 and milk protein expression. Scale bars: 50 μM. Red arrows indicate abnormal milk production in *Lbh*-deficient glands.

Fig. S4: Abnormal mammary epithelial cell morphology and basal-luminal lineage differentiation in ubiquitous *Lbh*–deficient mice. (A) H&E analysis of 8 week-old *R26-Cre*;*Lbh*$^{+/+}$ wild type (WT) and *R26-Cre*;*Lbh*$^{loxP/loxP}$ mammary glands. Note the abnormal basal cell morphology (red arrow) and thickening of the luminal epithelium (red arrowhead) in *Lbh*-deficient glands compared to WT (black arrow = basal epithelium; black arrowhead = luminal epithelium). (B) IHC showing decreased basal Keratin 5 (K5) expression (red arrow) in *R26-Cre;Lbh*$^{loxP/loxP}$ mammary glands, whereas luminal Keratin 8 (K8) expression did not detectably change relative to WT glands. (C) However, both, the intensity and number of luminal cells staining positive for ERα and its target gene, PR, were markedly increased (red arrowheads) in *Lbh*-deficient glands, as revealed by IHC analysis. (B,C) Scale bars; 25 μm. Close-ups on individual areas (black boxes) are shown. (D) qPCR analyses of *Lbh* and basal-luminal lineage marker expression in FACS sorted luminal (CD29^{lo}CD24^{hi}) and basal (CD29^{hi}CD24^{+}) MEC populations from *R26-Cre*;*Lbh*$^{+/+}$ WT and *R26-Cre;Lbh*$^{loxP/loxP}$ glands. Values were normalized to *Gapdh* and represent the mean ± SEM (n=3 mice per genotype). *$p<0.05$; **$p<0.01$; ***$p<0.001$; NS = non-significant.

Fig. S5: Ubiquitous inactivation of *Lbh* reduces basal MaSC frequency, activity and differentiation potential. (A) Histogram showing the percentages (%) of luminal CD29^{lo}CD24^{hi} and basal CD29^{hi}CD24^{+} subpopulations from 8-wk-old *R26-Cre*;*Lbh*$^{+/+}$ wild type (WT) and *R26-Cre;Lbh*$^{loxP/loxP}$ mutant mammary glands. **$p<0.01$; *Lbh*-deficient vs. WT mice (n=4 animals per group). (B-C) Mammosphere assays using single cell suspensions of freshly isolated (B) unsorted mammary cells, and (C) FACS sorted luminal (CD29^{lo}CD24^{hi}) and basal (CD29^{hi}CD24^{+}) subpopulations, as indicated. Values represent mean ± SD (n=4 animals per group); **$p<0.01$. (D) IF images of differentiation-induced primary mammospheres derived from CD29^{hi}CD24^{+} basal MaSC populations of WT and *Lbh*–deficient glands (see C) stained with antibodies for basal (K5; red) and luminal (K8; green) markers, as quantified in E). Scale bar; 100 μm. (E) Histogram showing the percentages (%) of K5^{+} basal (black), K8^{+} luminal (white), and K5^{+}/K8^{+} double-

positive progenitor cells (grey) after 5 days of differentiation. These percentages were derived from counting cells in 10 differentiated spheres from n=3 animals per genotype ($p<0.05$).

SUPPLEMENTARY FIGURES

FIGURE S1

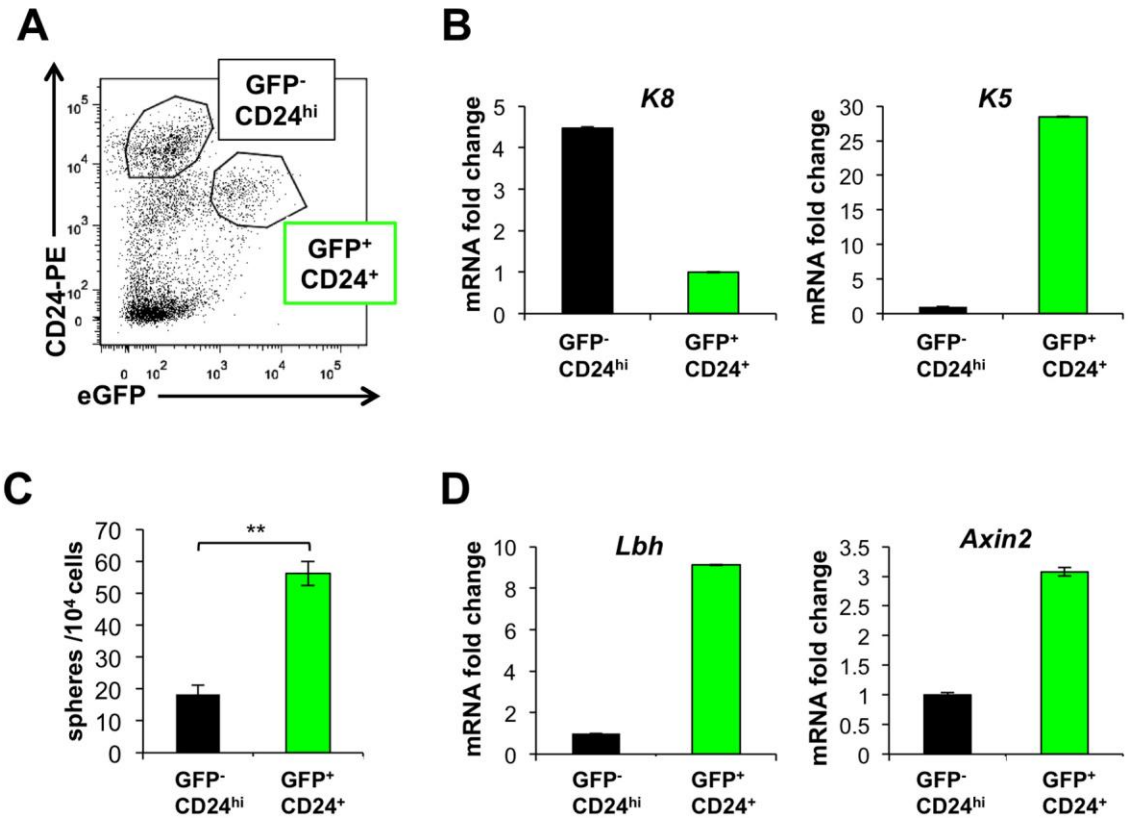

FIGURE S2

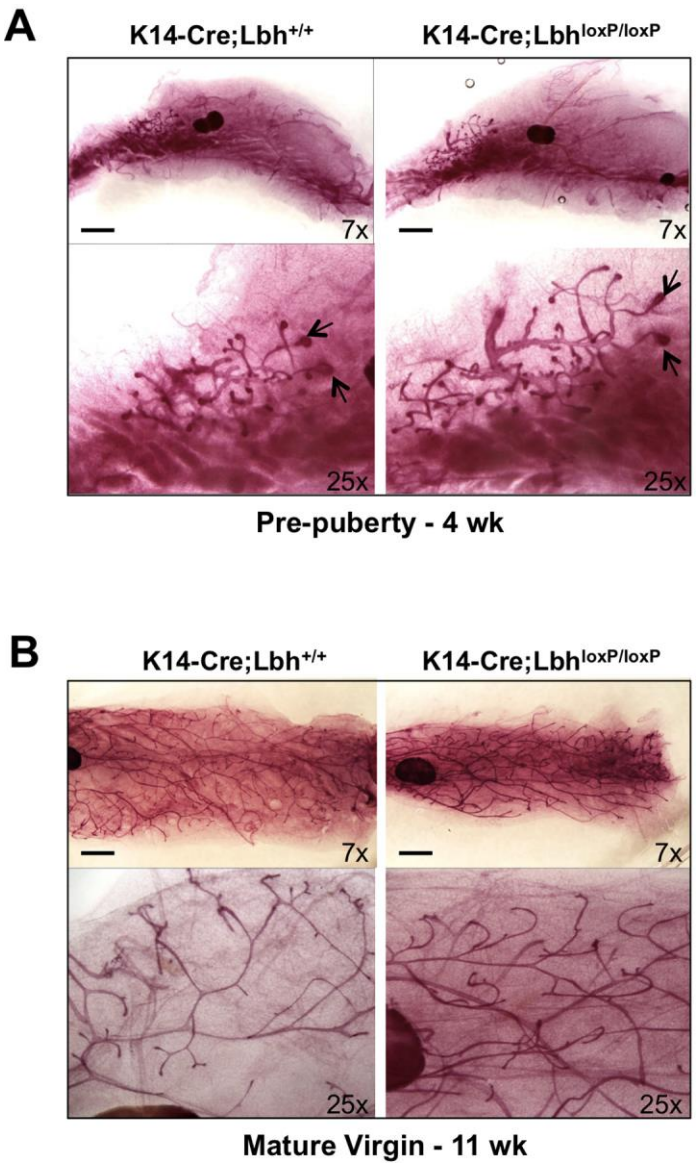
A
K14-Cre;Lbh+/+
K14-Cre;LbhloxP/loxP
7x
7x
25x
25x
Pre-puberty - 4 wk
B
K14-Cre;Lbh+/+
K14-Cre;LbhloxP/loxP
7x
7x
25x
25x
Mature Virgin - 11 wk

FIGURE S3

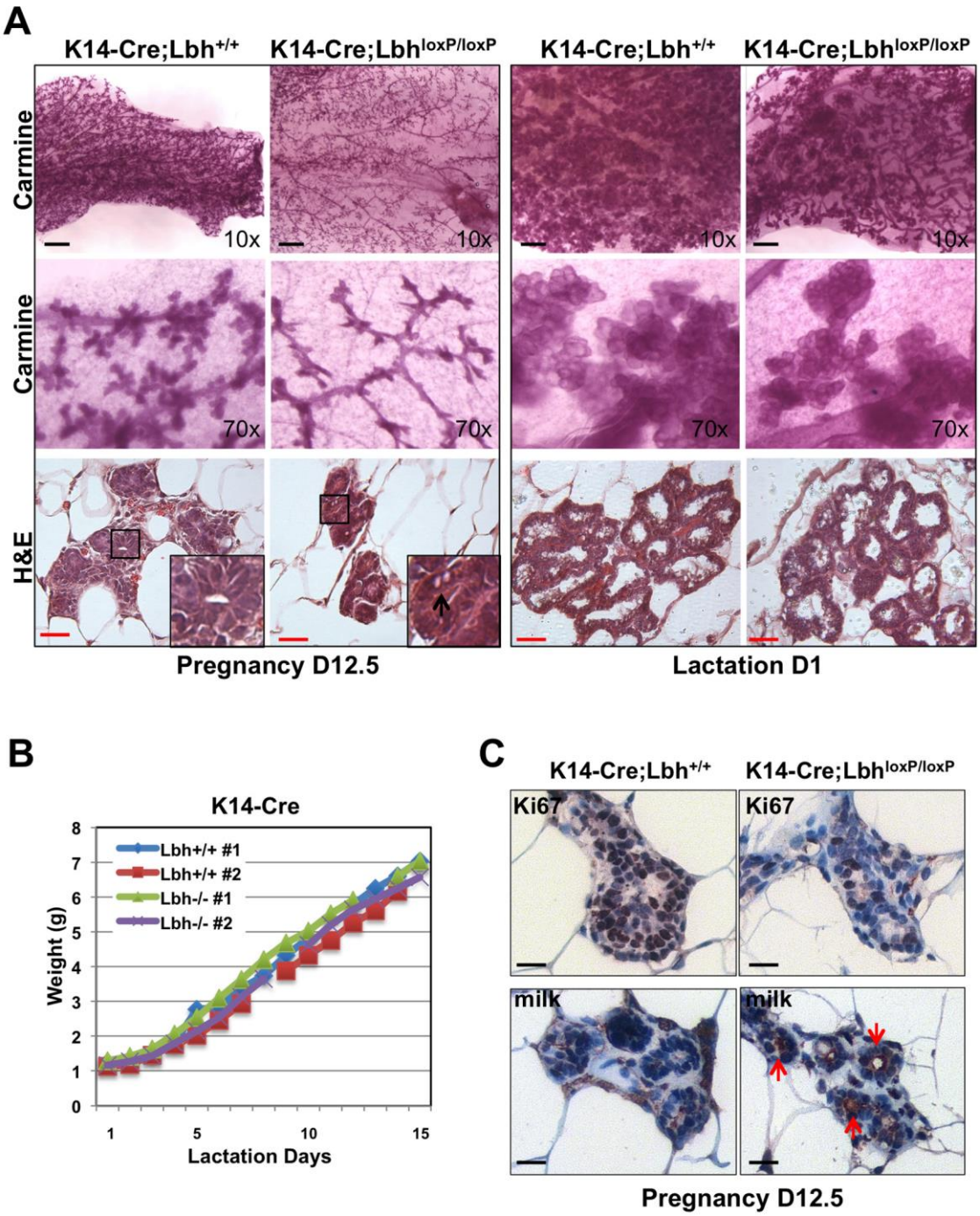
A
K14-Cre;Lbh+/+
K14-Cre;LbhloxP/loxP
K14-Cre;Lbh+/+
K14-Cre;LbhloxP/loxP
Carmine
Carmine
H&E
10x
70x
Pregnancy D12.5
Lactation D1
B
K14-Cre
Lbh+/+ #1
Lbh+/+ #2
Lbh-/- #1
Lbh-/- #2
Weight (g)
Lactation Days
C
K14-Cre;Lbh+/+
K14-Cre;LbhloxP/loxP
Ki67
milk
Pregnancy D12.5

FIGURE S4

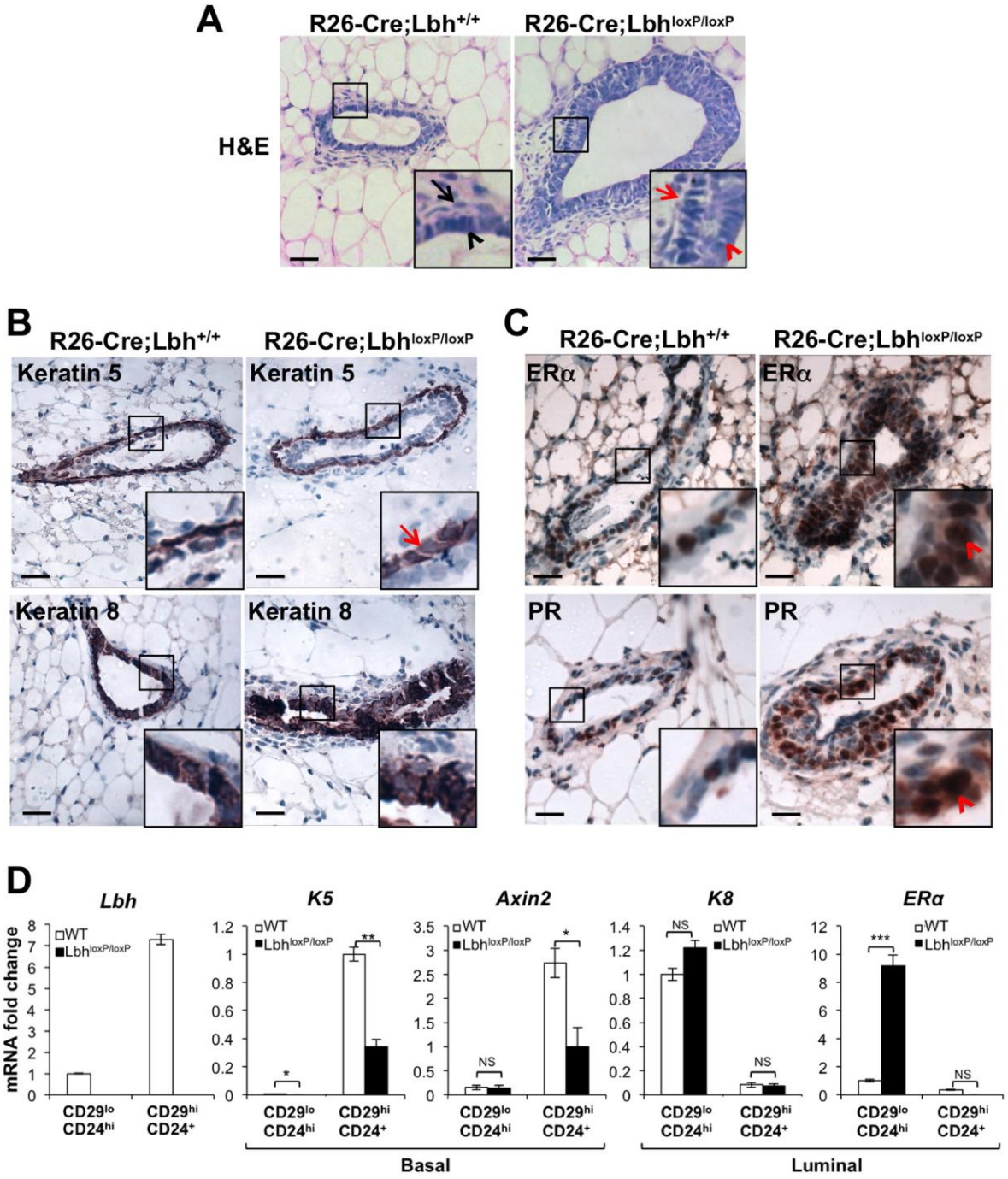
A
R26-Cre;Lbh+/+
R26-Cre;LbhloxP/loxP
H&E
B
R26-Cre;Lbh+/+
R26-Cre;LbhloxP/loxP
Keratin 5
Keratin 5
Keratin 8
Keratin 8
C
R26-Cre;Lbh+/+
R26-Cre;LbhloxP/loxP
ERα
ERα
PR
PR
D
Lbh
K5
Axin2
K8
ERα
mRNA fold change
WT
LbhloxP/loxP
CD29lo CD24hi
CD29hi CD24+
Basal
Luminal
NS
*
**
***

FIGURE S5

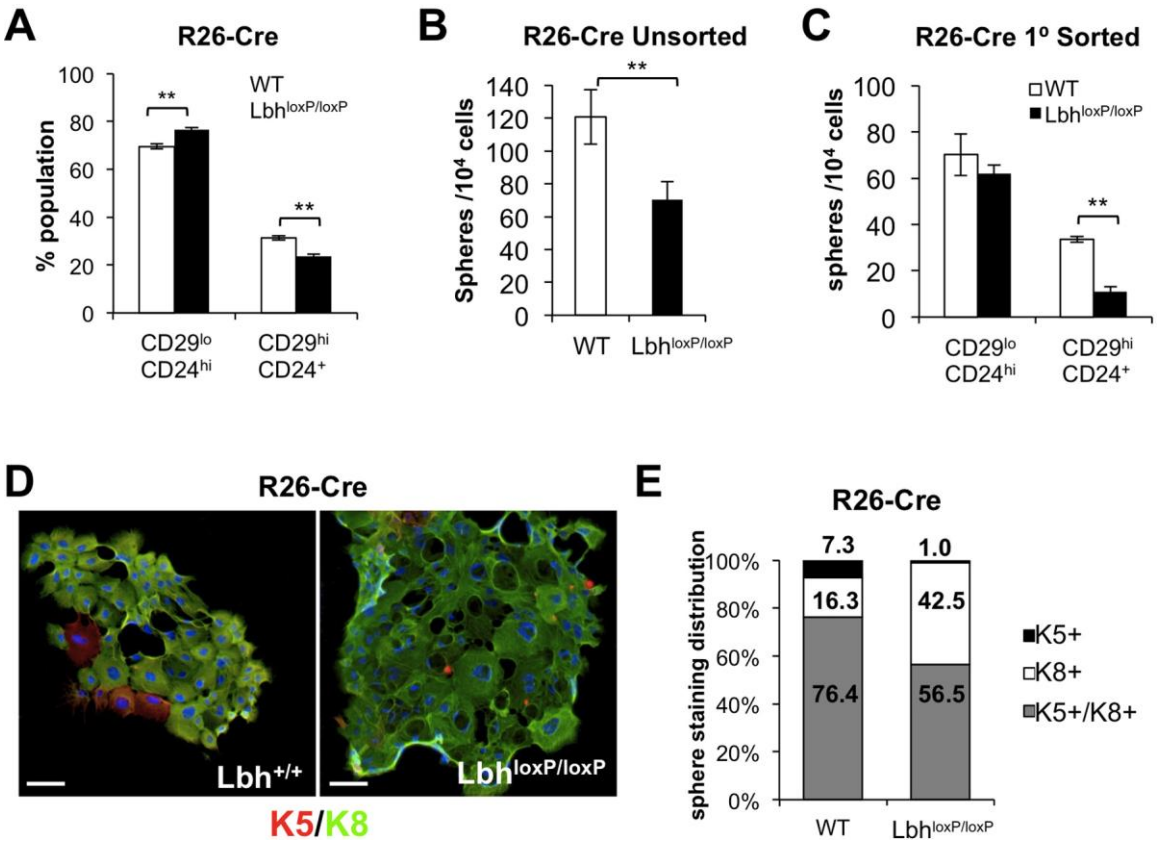
A
R26-Cre
% population
WT
Lbh loxP/loxP
CD29lo CD24hi
CD29hi CD24+
B
R26-Cre Unsorted
Spheres /10⁴ cells
WT
Lbh loxP/loxP
C
R26-Cre 1º Sorted
spheres /10⁴ cells
WT
Lbh loxP/loxP
CD29lo CD24hi
CD29hi CD24+
D
R26-Cre
Lbh+/+
Lbh loxP/loxP
K5/K8
E
R26-Cre
sphere staining distribution
7.3
16.3
76.4
1.0
42.5
56.5
K5+
K8+
K5+/K8+
WT
Lbh loxP/loxP